

Discreteness effects on the double-quadratic kink

P. Tchofo Dinda, R. Boesch, and E. Coquet

Laboratoire des Ondes et Structures Cohérentes, 6 Boulevard Gabriel, 21000 Dijon, France

C. R. Willis

Department of Physics, Boston University, 590 Commonwealth Avenue, Boston, Massachusetts 02215

(Received 16 December 1991; revised manuscript received 9 March 1992)

We study the static and dynamic properties of a kink in a chain of harmonically coupled atoms on a double-quadratic substrate. We treat intrinsically the lattice discreteness without approximation and demonstrate that the stable kink does not cause a phase shift of the phonons, and relate this result to Levinson's theorem. Using a recently developed projection-operator approach, we derive exact equations of motion for the kink center of mass, X , and coupled field variables. With neglect of radiation, a zeroth-order expression is obtained for the frequency with which the trapped kink oscillates in the Peierls-Nabarro well, and we show that the frequency lies in the phonon band. Consequently, we show that the effects of discreteness on the double-quadratic kink manifest themselves in surprisingly different ways than in a typical discrete kink-bearing system, i.e., the center-of-mass motion of a trapped double-quadratic kink is a quasimode in the same sense as is the shape mode of the sine-Gordon kink [R. Boesch and C. R. Willis, *Phys. Rev. B* **42**, 2290 (1990)]. We solve numerically the collective-variable equations of motion for the trapped and untrapped regimes of the discrete kink motion, and compare the results to those found for various other models.

I. INTRODUCTION

The many one-dimensional (1D) nonlinear lattices that give rise to energy-localization effects—and hence support stable kink structures such as the sine-Gordon (SG),^{1–6} the double Sine-Gordon,^{7,8} the ϕ^4 ,^{9–15} the double-quadratic,^{16–24} and the multiquadratic²⁵ systems—have given rise to a large amount of theoretical development owing to the interest in condensed matter and particle physics in their behavior as model systems. For example, areas of application of the SG model in condensed matter include dislocation lines in imperfect crystals,²⁶ ion motion in some superionic conductors,²⁷ and charge-density waves in metals.²⁸

Various models assume for an order parameter the position of a particle in a double-well substrate potential (e.g., the macroscopic polarization in ferroelectric and antiferroelectric crystals or the position of a proton in a hydrogen bonded system). Two common double-well potentials are the ϕ^4 and the double-quadratic (DQ) potential.

The ϕ^4 potential has received a great deal of attention^{9–15} as a model for domain walls in displacive phase transitions and has also proved useful in the study of protonic conductivity in hydrogen bonded systems.¹³ In the continuum limit this model gives rise to a nonlinear wave equation, which admits large-amplitude solitary wave or soliton solutions that retain their shape during propagation.

The DQ potential, on the other hand, consists of two displaced parabolas whose form allows one to proceed quite far in “analytical” investigations. The analytic tractability makes the DQ model attractive, for instance,

in the study of interactions between ferroelectric domain walls with external fields.^{25,23} The DQ model is especially attractive in the discrete case (since closed-form static solutions exist), such as in the study of the dynamics of a thermal ensemble of metastable structures,¹⁶ or the study of the static structure phase diagram of nonlinear lattices.^{17–20} Furthermore, the commensurate-commensurate or commensurate-incommensurate phase transitions, which appear in DQ systems with first- and second-neighbor interactions,^{17–22} involve the propagation of the so-called localized phase fronts along the lattice. The phase fronts have already been observed in various materials, e.g., LiIO_3 (Ref. 29) and KD_2PN_4 .³⁰ In a particular (static) phase, the fronts are nonpropagating, or fixed, and the phase can be regarded as a succession of a finite number of domain walls which make up the periodic unit cell. In this spirit, a simple formalism²² was developed recently for describing commensurate phases in 1D discrete DQ systems, and the discrete static solutions for particle positions as a function of the distances between domain walls were found. The formulation²² explicitly exhibits variables that are natural for setting up a particlelike description of the system. Those variables are the distances between the domain walls, or, equivalently, their positions, which can hence be treated as Hamiltonian dynamical variables. Such a particlelike, or collective variable, treatment would be of great interest for the study of the dynamics of collective entities such as phase fronts, and in general, the dynamics of phase transitions, which involve a modification of the distances between the domain walls. It is, therefore, interesting to examine, as a step in this direction, a discrete DQ chain with a single kink (domain wall) in a

collective-variable context where the collective variable represents the center of mass of the kink.

In the present paper we focus on the discrete DQ model with only nearest-neighbor interactions and show that the discreteness effects in this system are atypical and do not fit into the general picture that describes behavior found in other discretized field theories. For instance, the center-of-mass mode usually lies in the gap of the systems's excitation spectrum if the kink is trapped. In the discrete DQ model, however, we find the interesting result that the mode associated with the center-of-mass motion of a trapped kink *never* lies in the gap, and in this respect differs from all other known nonintegrable discrete field theories. Moreover, since the DQ kink exists, we would expect there to be a phase shift of a phonon as it traverses the kink. On the other hand, since there is no mode in the gap (i.e., no bound state, see Sec. II B below), Levinson's theorem¹³—which relates the phase shift through a scattering potential to the number of bound states supported by the scattering potential—predicts that there should be no phase shift. We resolve the apparent contradiction in Sec. II B. We show in the present paper that the DQ field is a candidate for studying the dynamic properties of systems in which the domain walls do not induce phase shift for phonons upon passage through the crystal.

We introduce into the discrete DQ system the collective variable X , which represents the position of the center of mass of the kink, and we obtain exact closed-form expressions for the static kink profile when the kink is located at symmetry points along the chain, and the kink's energy. We determine the spatial dependence of the Peierls-Nabarro (PN) potential and derive analytically a zeroth-order (neglecting radiation) expression for the frequency with which the trapped kink oscillates in the PN well, and we show that this frequency lies in the phonon band. To facilitate the calculation, we employ a projection-operator approach¹ in order to derive the equations of motion governing the evolution of the collective variable X . Such an approach was shown¹ to be an expedient equivalent to the Dirac-bracket theory³² of constrained Hamiltonian systems making the derivation of the collective-variable equations of motion extremely simple.

In order to determine the effects of the phonon field on the dynamics of the kink's center of mass, we numerically solve the collective-variable equations of motion for various initial conditions leading to trapped and untrapped motion. We find that the DQ kink behaves quite differently from the discrete ϕ^4 of SG kink in that, as soon as the DQ kink begins a trapped oscillatory motion, the frequency of oscillation of its center of mass—that is, the PN frequency—appears inside the phonon band and thus makes direct resonance with the phonon modes, in contrast to the ϕ^4 (Ref. 11) or SG (Ref. 2) kink for which the PN frequency is initially located in the gap below the phonon band. Consequently, the DQ kink significantly radiates away energy and the PN frequency continually decreases in time, whereas for the ϕ^4 and SG models the frequency is an increasing function of time. Also, unlike the ϕ^4 and SG models, the trapped DQ kink ultimately

reaches a steady state in which the ensuing oscillatory motion is almost perfectly harmonic with frequency very close to the lower phonon band edge, and the kink radiates phonons only weakly. Such behavior is characteristic of a localized quasimode. It was recently shown³³ that the internal or shape oscillation of a continuum SG kink is also a quasimode having a frequency that lies in the phonon continuum, is a monotonically decreasing function of time, and ultimately oscillates very close to the edge of the phonon continuum.

In the following section we define the DQ model under consideration and in Sec. II B we calculate the exact static solutions for the stable and unstable kink profiles, and the corresponding energies, and we examine the frequency spectrum of the system. Section II C is devoted to the determination of the X dependence of the PN potential, and in Sec. II D we perform the molecular-dynamics simulations of the motion of a trapped kink. We derive the collective-variable equations of motion in Sec. III A, obtain an expression for the zeroth-order PN frequency in Sec. III B, and in Sec. III C we numerically solve the collective-variable equations of motion. We conclude in Sec. IV.

Throughout the paper, our calculations treat intrinsically the lattice discreteness so that no continuum limit approximation is required.

II. STATIC AND DYNAMIC PROPERTIES

A. The model

The system under consideration is a one-dimensional chain of harmonically coupled particles governed by the following Hamiltonian:

$$\mathcal{H} = \sum_n \frac{1}{2} m \dot{u}_n^2 + \frac{1}{4} K_0 \sum_n [(u_n - u_{n-1})^2 + (u_n - u_{n+1})^2] + \frac{1}{2} m \omega_0^2 \sum_n (|u_n| - a)^2, \quad (2.1)$$

where u_n denotes the position of the n th particle measured from the center peak of the local substrate potential; $\pm a$ locate the two minima of the potential. The constant ω_0 represents the limiting frequency of infinite-wavelength phonons. The first term in Eq. (2.1) represents the kinetic energy carried by the displacement field (a dot denotes a time derivative), and the second term is the strain energy arising from the harmonic coupling with coupling constant K_0 between adjacent particles. Note that we have used here a symmetrized form of the energy per site in which half the coupling energy of a particle with its two neighbors is introduced, hence the factor $\frac{1}{4}$. The third term represents the substrate potential. Introducing the dimensionless position coordinate $Q_n = u_n/a$, the Hamiltonian becomes

$$H \equiv \frac{\mathcal{H}}{A} = l \left[\sum_n \frac{1}{2} \dot{Q}_n^2 + \frac{1}{4} \frac{C_0^2}{l^2} \sum_n [(\mathcal{Q}_n - \mathcal{Q}_{n-1})^2 + (\mathcal{Q}_n - \mathcal{Q}_{n+1})^2] + \frac{1}{2} \omega_0^2 \sum_n (|\mathcal{Q}_n| - 1)^2 \right], \quad (2.2)$$

in units of $A = ma^2/l$; $C_0^2 = K_0 l^2/m$ is the limiting velocity of the kink, and $l > 2a$ denotes the length of the unit cell in the chain.

The potential energy is defined by

$$E_V = l \left[\frac{1}{4} K_1 \sum_n [(\mathcal{Q}_n - \mathcal{Q}_{n-1})^2 + (\mathcal{Q}_n - \mathcal{Q}_{n+1})^2] + \frac{1}{2} \omega_0^2 \sum_n (|\mathcal{Q}_n| - 1)^2 \right], \quad (2.3)$$

where $K_1 = C_0^2/l^2$. We introduce the *discreteness parameter* γ ,

$$\gamma = \frac{C_0}{\omega_0 l} \equiv \frac{d}{l}, \quad (2.4)$$

which serves as a measure of the kink length relative to a lattice spacing l , and hence a measure of the importance of discreteness effects.

B. Single-kink profile-exact static solutions

The static structure of the system is obtained by solving $\partial E_V / \partial \mathcal{Q}_n = 0$, where E_V is defined in Eq. (2.3), which gives us the following equilibrium equation:

$$\mathcal{Q}_{n-1} + 2B\mathcal{Q}_n + \mathcal{Q}_{n+1} = g(n), \\ g(n) = -\sigma_n / \gamma^2, \quad B = -1 - 1/(2\gamma^2), \quad (2.5)$$

where $\sigma_n = \text{sgn}(\mathcal{Q}_n)$ represents a given sequence of Ising variables (± 1) describing the occupied side of the double-well substrate potential at each site of the chain. Equation (2.5) is an inhomogeneous difference equation which can be solved exactly for an arbitrary sequence σ_n .^{17,19,34} The general solution is written

$$\mathcal{Q}_n = (\nu - 1/\nu)^{-1} \sum_{j=-\infty}^{j=+\infty} g(n+j) \nu^{|j|}, \\ \nu = 1 + (1/2\gamma^2) [1 - (1 + 4\gamma^2)^{1/2}]. \quad (2.6)$$

In order to obtain a kink solution that explicitly exhibits all the equilibrium configurations, we introduce the variable X — which represents the position of the kink relative to a lattice spacing l —by defining the sequence σ_n as follows:

$$\sigma_n \equiv \sigma(n-X) = \text{sgn}(n-X), \quad \sigma(0) = 0. \quad (2.7)$$

Then, performing the sums of the infinite series in Eq. (2.6), we obtain the following solution:

$$\Phi_n \equiv \mathcal{Q}_n = \sigma(n-X) + \left[\frac{\nu-1}{\nu+1} \sigma(R_X) - \sigma(n-X) \right] \nu^{|\text{Int}(X)-n|}, \quad (2.8)$$

where $\text{Int}(X)$ represents the integral part of X , $R_X = X - \text{Int}(X)$, $-1 < R_X < 1$.

Substitution of Eq. (2.8) in Eq. (2.3) yields the kink energy at equilibrium

$$E_K = \frac{E_{K_0}}{2\gamma(1+4\gamma^2)^{1/2}} [1 - \sigma^2(R_X) + 4\gamma^2], \quad E_{K_0} = C_0 \omega_0. \quad (2.9)$$

We henceforth consider $X > 0$, so that $0 \leq R_X < 1$. Thus, the static solutions Φ_n and E_K in Eqs. (2.8) and (2.9), respectively, show that for a single kink there are exactly two solutions for the equilibrium equation (2.5), since $\sigma(R_X)$ is either equal to 1 or 0, depending on whether $R_X \neq 0$ or $R_X = 0$. The solution with $R_X \neq 0$ corresponds to a kink centered midway between two particles, implying that R_X is not arbitrary if $R_X \neq 0$, but takes the value $R_X = \frac{1}{2}$. Equation (2.9) shows that this solution corresponds to an energy minimum, that is, the stable kink Φ_n^s . The kink solution with $R_X = 0$, Φ_n^u , corresponds to the higher-energy configuration [see Eq. (2.9)] and is unstable. This solution corresponds to a kink that is centered exactly on a particle of the chain. An elementary algebraic manipulation gives us

$$\Phi_n^s = \sigma(n-X) [1 - Z_\nu \nu^{|X-n|}], \\ Z_\nu = \frac{2\nu^{1/2}}{(1+\nu)}, \quad X = m + \frac{1}{2}, \quad m = 0, 1, 2, \dots \quad (2.10)$$

$$\Phi_n^u = \sigma(n-X) [1 - \nu^{|X-n|}], \quad X = m, \quad m = 0, 1, 2, \dots$$

Note that the solution (2.10) fulfills the self-consistency condition $\sigma_n = \text{sgn}(\mathcal{Q}_n)$ at each site of the lattice for all finite values of γ . This solution generalizes the results obtained in previous work,^{16-19,34} in that this solution provides, in addition to the stable kink profile Φ_n^s , an analytical expression for the unstable kink Φ_n^u .

Figure 1, which gives plots of different stable kink profiles Φ_n^s for different values of the discreteness parameter γ , shows in general that when $\gamma \gg 1$ the coupling between sites is so strong that the variation of Φ_n^s from site to site is very small. This corresponds to the so-called dispersive (or continuum) limit. The spatial extension of the kink decreases continuously as γ decreases. As γ decreases below unity, Φ_n^s approaches a step function.

Furthermore, it is interesting to note that in the dispersive limit ($\gamma \gg 1$), $\nu \sim 1 - 1/\gamma$ [see Eq. (2.6)], then $Z_\nu \sim 1$ [see Eqs. (2.10)], so that

$$\Phi_n^s \sim \sigma(n-X) [1 - \nu^{|X-n|}] = \Phi_n^u.$$

As $\nu \sim 1 - 1/\gamma \sim e^{-1/\gamma}$, then the static solutions becomes

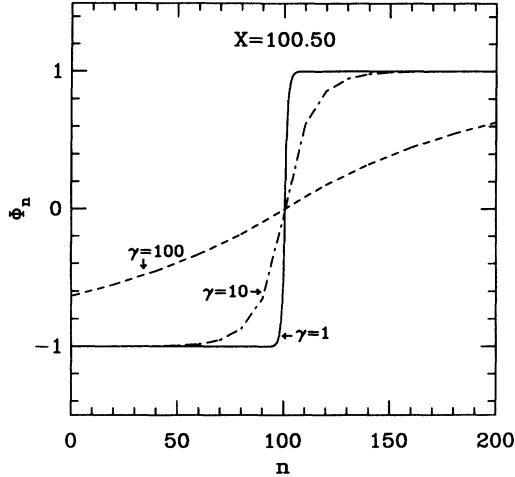


FIG. 1. Kink profile Φ_n for various values of the discreteness parameter γ . Note the increase in the spatial extension of the kink as γ increases.

$$\Phi_n^s \sim \Phi_n^u \sim \sigma(n-X)[1 - e^{-|X-n|/\gamma}] \quad (\gamma \gg 1). \quad (2.11)$$

Substituting $\gamma = d/l$ and $x = nl$ into (2.11), we recover precisely the “continuum” solution obtained by Trullinger and DeLeonardis,²⁴ translated by

$$\bar{X} = lX, \quad (2.12)$$

that is the position of kink in the lattice. Furthermore, note that the PN barrier height E_{PN} , defined as the energy required to move the kink by one lattice spacing, is simply given by

$$E_{PN} \equiv E_K(R_X=0) - E_K(R_X=\frac{1}{2}) = (Z_v - Z_v^{-1})E_{K_0}.$$

Also note that for $\gamma \gg 1$,

$$E_K(R_X=\frac{1}{2}) \approx E_K(R_X=0) \rightarrow \omega_0 C_0 = E_{K_0},$$

where E_{K_0} is in fact the kink rest energy of the “continuum” kink, obtained by Trullinger and DeLeonardis.²⁴ The PN barrier vanishes in the displacive limit.

We now turn our attention to an examination of small oscillations in the presence of a kink. The equations of motion for the *infinite* chain are written

$$\begin{aligned} \ddot{Q}_n - K_1 \Delta_2 Q_n + \omega_0^2 V_s' &= 0, \\ \Delta_2 h_n &= (h_{n-1} + h_{n+1} - 2h_n), \\ V_s &= \frac{1}{2}(|Q_n| - 1)^2. \end{aligned} \quad (2.13)$$

Throughout the paper, we consider a chain with a finite number of particles, so that only first difference is needed for an end particle. In order to examine small oscillations in the presence of an equilibrium kink Φ_n^{eq} , we consider

$$Q_n(t) = \Phi_n^{\text{eq}} + \vartheta_n(t),$$

where $\vartheta_n(t) = \epsilon \lambda_n \exp(-i\omega t)$ (ϵ is a small parameter) and $\Phi_n^{\text{eq}} = \Phi_n^s$, or $\Phi_n^{\text{eq}} = \Phi_n^u$. The linearization about Φ_n^{eq} yields

$$\ddot{\vartheta}_n - K_1 \Delta_2 \vartheta_n + \omega_0^2 V_s''(\Phi_n^{\text{eq}}) \vartheta_n = 0, \quad (2.14)$$

where

$$V_s''(\Phi_n^{\text{eq}}) = 1 - 2\delta(\Phi_n^{\text{eq}}) \equiv 1 - 2\delta(X - n) \quad (2.15)$$

is the “scattering” potential. [Note that the δ function appears in (2.15) only if $\Phi_n^{\text{eq}} = \Phi_n^u$, that is, if X is an integer.] We present separately the cases $\Phi_n^{\text{eq}} = \Phi_n^s$ and $\Phi_n^{\text{eq}} = \Phi_n^u$.

(i) For $\Phi_n^{\text{eq}} = \Phi_n^s$ [$X = \frac{1}{2}$, $V_s''(\Phi_n^{\text{eq}}) = 1$], the spectrum consists entirely of plane-wave phonons and the dispersion law^{23,24,16} is expressed in terms of our discreteness parameter as

$$\omega_k^2 = \omega_0^2 [1 + 4\gamma^2 \sin^2(k/2)], \quad (2.16)$$

where k is the wave vector associated with the frequency ω_k . Therefore, there is no mode in the gap and, consequently, there is no bound state associated with the motion of the kink’s center of mass in the PN potential. By Levinson’s theorem,³¹ there is no phase shift of a phonon as it traverses the kink. The kink is *linear* because the coupling potential as well as the substrate potential are harmonic [the substrate potential is piecewise harmonic], unlike the discrete SG or ϕ^4 models which are characterized by nonlinear substrate potentials. When linearizing about the SG and ϕ^4 kink solution, one obtains a nonlinear scattering potential acting on the phonons, and a phonon suffers a phase shift upon passing through the kink. For the DQ model, the kink is a *linear object* consisting only of phonons; consequently the effective frequency with which the kink oscillates in the PN well is necessarily in the phonon band, as shown by Eq. (2.16), whereas for the SG (Ref. 2) or ϕ^4 (Ref. 11) models, the PN frequency is in the gap. We now consider the case $\Phi_n^{\text{eq}} = \Phi_n^u$ in an attempt to find whether or not there exists in the discrete system a mode, even an unstable one, that becomes the Goldstone mode in the continuum limit.

(ii) For $\Phi_n^{\text{eq}} = \Phi_n^u$, $V_s''(\Phi_n^{\text{eq}}) = 1 - 2\delta(X - n)$, and Eq. (2.14) becomes

$$-\omega^2 \lambda_n - K_1 \Delta_2 \lambda_n = -\omega_0^2 \{1 - 2\delta(X - n)\} \lambda_n. \quad (2.17)$$

Equation (2.17) takes the form of the Schrödinger equation for a particle in the presence of a δ -function potential well if and only if the kink is always centered exactly on a particle of the chain, that is, if X is an integer n_0 . In this case the presence of the kink provides a localized potential acting on the phonons, in the sense that the “phonon solutions” must be necessarily X dependent. We then assume solutions of the form

$$\begin{aligned} \lambda_n &= a_1(k) \exp\{i(n-X)k\} \\ &+ b_1(k) \exp\{-i(n-X)k\} \quad \text{as } n-X \rightarrow +\infty, \end{aligned} \quad (2.18a)$$

$$\begin{aligned} \lambda_n &= a_2(k) \exp\{i(n-X)k\} \\ &+ b_2(k) \exp\{-i(n-X)k\} \quad \text{as } n-X \rightarrow -\infty, \end{aligned} \quad (2.18b)$$

where the $a_i(k)$ and $b_i(k)$ ($i=1,2$) are arbitrary functions of k . Substituting Eqs. (2.18) into (2.17), we obtain

$$[-\omega^2 + \omega_0^2 + 4K_1 \sin^2(k/2)]\lambda_n = 2\omega_0^2 \delta(n-X)\lambda_n, \quad (2.19)$$

For $n \neq X \equiv n_0$ the dispersion relation is satisfied; consequently Eq. (2.19) is satisfied if and only if

$$\lambda_{n_0} = 0. \quad (2.20)$$

Using Eqs. (2.20) and (2.17), a little more algebra shows that the solution of Eq. (2.17) is

$$\lambda_n = A_k \sin\{(n-X)k\}, \quad (2.21)$$

where A_k is a normalization constant. However, this solution is not localized about the kink and corresponds to a state in which the kink is always centered exactly on a particle of the chain. Consequently, a mode associated with the motion of the kink's center of mass is not defined in this case, since the center of mass of the kink X does not move off the top of the PN potential. If it moves, the Schrödinger-like form of Eq. (2.17) is lost and one finds oneself in the previous case $\Phi_n^{\text{eq}} = \Phi_n^s$. These statements, in addition to the symmetry of the solution (2.21), show that the state described by (2.21) does not become the Goldstone mode in the continuum limit.

The above analysis clearly shows that there is no continuous transition from the trapped regime of the discrete behavior (in which the kink oscillates in the PN potential) to the continuum behavior (in which the kink freely translates), in contrast to the SG or the ϕ^4 systems, where there exist discrete localized PN modes whose frequencies continuously go to zero as the continuum limit is approached.

C. PN potential

We now study the shape of the PN potential. In order to obtain the X dependence of the PN potential, we make use of a quasistatic solution for the kink profile $\Phi_n^e(X)$, which is valid for all X . $\Phi_n^e(X)$ is quasistatic in the sense that the kink is held fixed at arbitrary X by applying an external force on a particle near the kink's center. The solution $\Phi_n^e(X)$ is found numerically by then letting the system relax subject to the external force. The chain is considered to be relaxed when the maximum force on any particle in the chain is not greater than $10^{-12}K_1l$.

We see that the expression of the solutions $\Phi_n^s(X)$ and $\Phi_n^u(X)$ [in Eqs. (2.10)] differs solely by the term Z_ν which is present in $\Phi_n^s(X)$, so that we can postulate that the quasistatic profile for arbitrary X has the following form:

$$\psi_n(X) = \sigma(n-X)[1 - \nu^{|X-n|} Z_\nu^{\phi(X)}], \quad (2.22)$$

where the function $\phi(X)$ must satisfy the following conditions. We require that $\psi_n(X)$ become the exact solutions $\Phi_n^s(X)$ for $X = m + \frac{1}{2}$ and $\Phi_n^u(X)$ for $X = m$, so that we must have

$$\phi(X) = 0, \quad R_X = 0,$$

$$\phi(X) = 1, \quad R_X = \frac{1}{2}.$$

The periodicity of the lattice requires that $\phi(X) = \phi(R_X)$, whereas the symmetry of the lattice requires $\phi(R_X)$ to be symmetric with respect to $R_X = \frac{1}{2}$, so that we must have

$$\phi(R_X) = \phi(1 - R_X).$$

A relatively simple expression that satisfies these conditions is

$$\phi(R_X) = [4R_X(1-R_X)]^{\rho(|R_X - 1/2|)}. \quad (2.23)$$

Of course, other choices for $\phi(R_X)$ are possible. The function ρ in Eq. (2.23) is obtained by requiring that

$$\psi_n(X) = \sigma(n-X)[1 - \nu^{|X-n|} Z_\nu^{[4R_X(1-R_X)]^\rho}] \quad (2.24)$$

minimize the functional Π , where

$$\Pi = \sum_n (\psi_n - \Phi_n^e)^2, \quad (2.25)$$

i.e., ϕ_n is a best fit to Φ_n^e . An empirical polynomial fit yields

$$\rho(\Gamma) = 12.294 - 48.495\Gamma + 91.334\Gamma^2 - 68.0878\Gamma^3, \\ \Gamma = |R_X - \frac{1}{2}|. \quad (2.26)$$

In order to see how good it is, we evaluate two measures of the correctness of ψ_n with ρ given by Eq. (2.26), namely Π in Eq. (2.25) and

$$\Lambda = \max(|\psi_n - \Phi_n^e|). \quad (2.27)$$

Scanning the range $0 \leq R_X < \frac{1}{2}$, we obtain, for different values of γ , the results which appear in Figs. 2. We see in Figs. 2 (a) and (b) that for $\gamma=1$, Λ and Π do not exceed 8×10^{-3} and 6.5×10^{-5} , respectively. The subsequent frames show that the agreement becomes better as

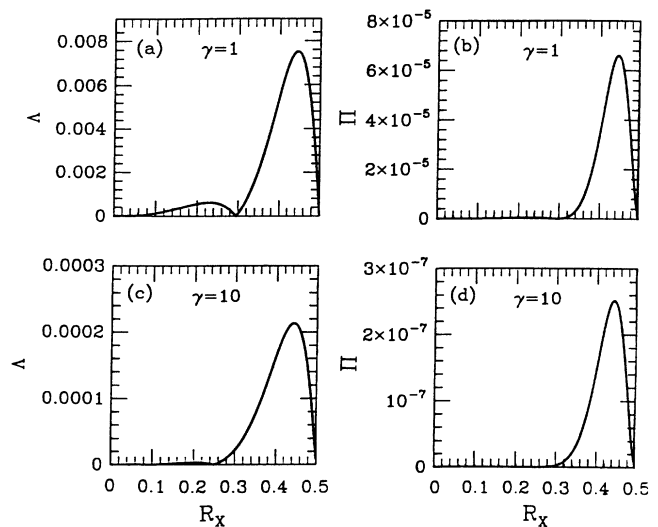


FIG. 2. Evaluation of the agreement between the approximate solution $\psi_n(X)$ and the exact quasistatic solution $\Phi_n^e(X)$. Maximum value of the static dressing Λ vs R_X , and value of the fit Π as a function of R_X . (a) and (b): for $\gamma=1$; (c) and (d): for $\gamma=10$. Simulation parameters are $\omega_0=1$, $C_0=3\gamma$, and $l=3$.

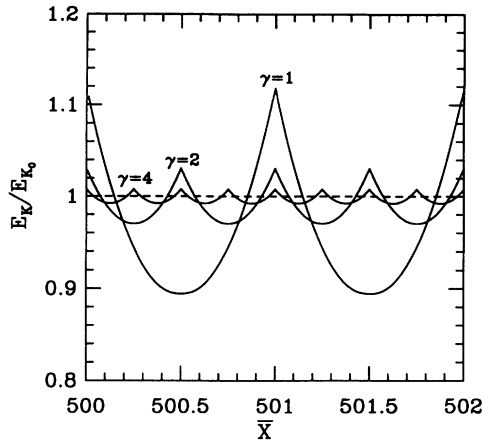


FIG. 3. The normalized PN potential as a function of X for different values of the discreteness parameter. The dashed line represents the continuum kink rest energy. Simulation parameters are $\omega_0=1$ and $C_0=1$.

γ increases, i.e., as one approaches the continuum limit. We also find that the difference $|E_K(\psi_n) - E_K(\Phi_n^e)|$ is the same order of magnitude as Π . We then conclude that in the context of the collective-variable approach, $\psi_n(X)$ provides an approximate but highly accurate representation of the shape of the kink for all X and becomes the exact solution $\Phi_n^u(X)$ or $\Phi_n^s(X)$ when $X=m$ or $X=m+\frac{1}{2}$.

Finally, we obtain the X dependence of the PN potential for any value of the discreteness parameter γ by substituting the solution $\psi_n(X)$ into the expression for the potential energy, Eq. (2.3). Figure 3 shows the shape of the normalized PN potential as a function of \bar{X} . We see that the PN potential of the DQ kink possesses the same type of discontinuity as the DQ substrate potential. This differs from the ϕ^4 (Ref. 11) and SG (Ref. 5) models for which the top of the PN potential is rather smooth.

D. Molecular-dynamics simulations, trapped case

We simulate the trapped motion of a kink by starting with a kink that is relaxed to unstable equilibrium at the top of the PN well; where $X(t=0) = \text{Int}(N/2) + \varepsilon$ and $\dot{X}(0)=0$, where ε is a very small deviation of the kink's center from the equilibrium position ($\varepsilon \sim 10^{-10}$), and N is the total number of particles of the chain; which yields the following initial conditions for the molecular-dynamics simulation (MDS): $Q_n(0) = \psi_n(X(0))$ and $\dot{Q}_n(0) = 0$. The kink then moves off the top of the PN well due to the small deviation ε and begins to oscillate. Hereafter the dynamical simulation time step Δt is chosen to conserve the energy of the system to an accuracy better than 0.1%; the total number of particles N and the total simulation time t_f are chosen such that we do not encounter phonons reflected from the ends of our system. We obtain the center of the kink from MDS (throughout the paper) by requiring the quasistatic kink profile $\psi_n(X)$ given by Eqs. (2.24) and (2.26) to be a best fit to the field variable $Q_n(t)$ (obtained from MDS) as follows:

$$\frac{d}{dX} \sum_n [Q_n(t) - \psi_n(X)]^2 = 0. \quad (2.28)$$

It is helpful to note that before solving Eq. (2.28), for X , we first estimate the approximate value of X , X_{LI} , via a linear interpolation,²

$$X_{\text{LI}} = \frac{Q_n}{Q_n - Q_{n+1}} + n, \quad Q_n < 0 \text{ and } Q_{n+1} > 0, \quad (2.29)$$

and then we obtain the solution X from Eq. (2.28) by simply scanning a small region neighboring X_{LI} . We define the velocity by $V(t) = \{X(t+\Delta t) - X(t)\} / \Delta t$.

We obtain from MDS the frequency of oscillations averaged over individual cycles of the kink's motion and show the result for $\gamma=1$ in Fig. 4. [The simulation parameters are $C_0=3$, $\omega_0=1$, $\Delta t = \pi/111.5$, $t_f \approx 1065$, $N=2000$.] We see in this figure that, as soon as the kink begins its motion, the PN frequency ω_{PN} lies in the phonon band, $\omega_{\text{PN}} \approx 1.07\omega_0$. Then ω_{PN} decreases to $\omega_{\text{PN}} \approx \omega_0$ after about ten oscillations, and finally remains essentially constant at ω_0 during the ensuing motion. This small variation of the PN frequency at the beginning of a large-amplitude oscillatory motion of a trapped DQ kink does not imply the presence of anharmonicity in the kink's motion, in contrast to SG and ϕ^4 , since no anharmonicity exists. The small variation in the PN frequency is due to the following reason: Since the PN frequency lies in the phonon band, it is then clear that the motion of the kink's center of mass is generated by a "packet of phonons." When the kink begins its motion, the PN frequency is initially slightly different from ω_0 , owing to the fact that a part of the phonons which contribute to the motion of the kink's center of mass is created at frequency $\omega \neq \omega_0$. Then the PN frequency decreases in time, which indicates that those phonons created at frequencies $\omega \neq \omega_0$ propagate away owing to their nonzero group velocities. The phonons created at frequency ω_0 , or nearly so, with a zero or small group velocity, cannot propagate

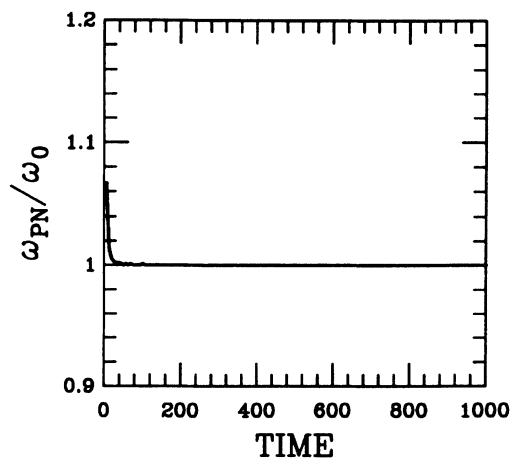


FIG. 4. Normalized PN frequency of trapped kink motion averaged over individual cycles. Simulation parameters are $V_0=0$, $\Delta t = \pi/111.5$, $\omega_0=1$, $C_0=3$, $l=3$, and $X_0 = N/2 + \varepsilon = 1000 + 10^{-10}$.

and therefore make up the oscillations of the kink at frequency $\omega_{\text{PN}} \approx \omega_0$ during the ensuing oscillatory motion.

The behavior observed for the SG (Refs. 2 and 3) or the ϕ^4 (Ref. 11) model is quite different; indeed these two models are characterized by the presence of anharmonicity in the kink's motion, which arises from the nonlinearity of the substrate potential. At the beginning of a large-amplitude oscillatory motion, the PN frequency for the SG or the ϕ^4 kink is small and located below the lower phonon band edge;^{3,11} this frequency increases in time as the kink radiates, in contrast to the DQ case, for which the PN frequency is initially inside the phonon band and decreases in time.

In Figs. 5(a) and 5(c), obtained for the same simulation data as for Fig. 4, we plot the molecular-dynamics results for the kink's position and the Poynting flux of the phonon radiation evaluated 25 particles away from the center of the kink, both as a function of time. The discrete definition of the Poynting flux S is²

$$S(n,t) = \left\{ \frac{Q_n(t+\Delta t) - Q_n(t)}{\Delta t} \right\} \{Q_{n+1}(t) - Q_n(t)\}.$$

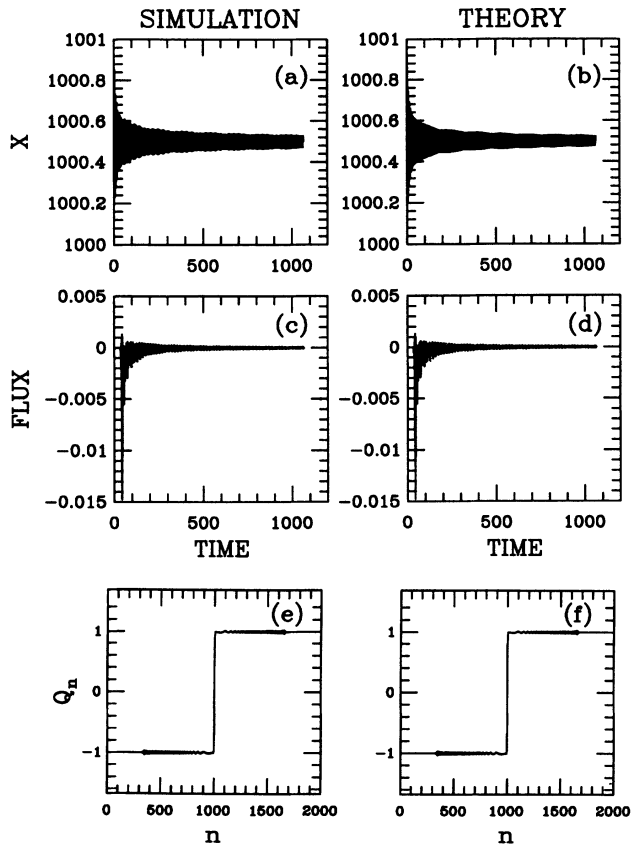


FIG. 5. Simulation and collective-variable theory for $\gamma=1$. (a) and (b): $X(t)$; (c) and (d): instantaneous Poynting's flux calculated 25 particles away from kink; (e) and (f): kink profile at the end of the total time of the calculations, that is, at $t=t_f \approx 1065$. Simulation parameters are the same as for Fig. 4, $\alpha=0$.

We see in Fig. 5(c) that when the kink begins its motion it significantly radiates away energy by emitting a large phonon packet. Its amplitude of oscillations then drops strongly in order to conserve energy [Fig. 5(a)]. Next the kink reaches a quasisteady state in which it radiates phonons weakly, and its amplitude decreases slowly. Furthermore, we point out that the large phonon packet emitted by the DQ kink at the beginning of its motion is not truly a bursting phenomenon such as that observed in the SG model.² In Ref. 2, the authors proposed a parametric coupling of the PN frequency in the gap to the radiation field. They showed that the bursting phenomenon occurs when harmonics of the PN frequency, which are previously below the lower phonon band edge and therefore not producing radiation, cross over up into the high-density-of-states region of the phonon band. These harmonics then act as a source of radiation by resonating with phonon modes, thereby producing a burst. It is important to mention that this mechanism results from the presence of anharmonicity in the kink's motion. For the DQ kink, a large phonon packet is emitted at the beginning of the kink's motion, but, in this case, the process results only from the radiation of the phonons created at frequencies $\omega \neq \omega_0$ and $\omega \neq \omega_\pi$, which propagate away owing to their nonzero group velocities. (Furthermore, it is important to note that we do not have exactly $\omega_{\text{PN}} = \omega_0$ during the quasisteady state simply because, although the radiation emitted by the kink is weak, it is not zero.)

We now consider the frequency spectrum obtained by performing a Fourier transform of the kink's motion.³⁵ The transform begins at $t \approx 1065$ (that is, about 500 kink oscillations after $t=0$). Figures 6(a) and 6(b) show the results obtained for the case $\gamma=1$ discussed above. The Fourier spectrum in Fig. 5(a) show that a group of about 30 center particles, from $n \approx 15$ up to $n \approx 35$, oscillate at frequencies $\omega \approx \omega_0$ and $\omega = 2.23\omega_0 \approx \omega_\pi$ (which corresponds to the upper phonon band edge $k=\pi$). Figure 6(b), which shows the relative amplitude of the Fourier transform for particles No. 25, consists of the two peaks ω_0 and ω_π . Note that the peak ω_π corresponds to a state in which two adjacent particles of the chain vibrate out of phase by π and therefore do not correspond to the oscil-

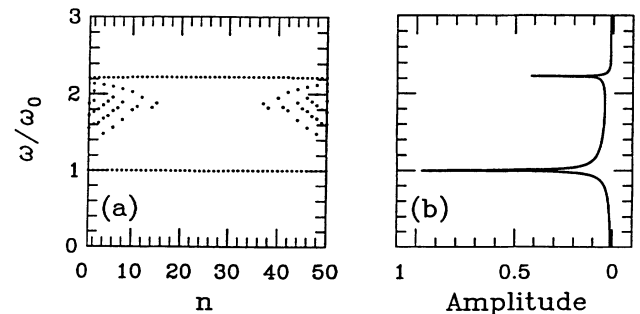


FIG. 6. Temporal Fourier transform of a trapped kink for $\gamma=1$. (a) Normalized frequency vs particle number for a cutoff value of 0.01. (b) shows the relative amplitude vs normalized frequency of the states in (a) for particle No. 25. Simulation parameters are the same as for Fig. 4.

lations of the kink center $X(t)$. The phonons created at this frequency cannot propagate, owing to their zero group velocity, and they are therefore present throughout the duration of the transform. The other pronounced phonon state $\omega \approx \omega_0$ corresponds to the effective frequency at which the kink's center of mass oscillates.

Thus, although the trapped DQ kink does not possess a rigorous nonlinear mode, its center-of-mass mode appears to be a quasimode, i.e., a mode in the same sense as is the shape mode of a SG kink.³³

III. COLLECTIVE-VARIABLE THEORY

A. Collective-variable equations of motion

We introduce the kink center-of-mass collective variable $X(t)$ in our system by introducing the ansatz

$$Q_n = f_n(X) + q_n, \quad (3.1)$$

where $f_n(X)$ is a suitably chosen function and q_n is then the remaining field such that the sum of $f_n(X)$ and q_n satisfies Eq. (3.1). The equation of motion in terms of the actual field Q_n is written [cf. Eq. (2.13)]

$$\ddot{Q}_n + \Delta Q_n - \omega_0^2 \sigma(Q_n) = 0, \quad (3.2)$$

where the difference Δ without a subscript is defined as

$$\Delta h_n = B_1 h_n - K_1 (h_{n-1} + h_{n+1}),$$

$B_1 = 2K_1 + \omega_0^2$. According to the projection-operator approach,¹ one needs to specify two constraints, and they are

$$C_1 = \langle f'_n(X) | q_n \rangle = 0, \quad C_2 = \langle f'_n(X) | p_n \rangle = 0, \quad (3.3)$$

where the bracket notation means sum over the particle index, and p_n is the momentum conjugate to q_n . The prime denotes the derivative with respect to the argument. The constraint C_1 determines the value of the collective variable X , which makes the function f_n a best fit to the actual field Q_n and in this way it gives the variable X its physical meaning. The constraint C_2 determines the momentum transformation, which yields a particle-like description of the dynamics. Substituting Eq. (3.1) into Eq. (3.2) yields

$$\ddot{X} f'_n + \dot{X}^2 f''_n + \ddot{q}_n + \Delta q_n + \Delta f_n - \omega_0^2 \sigma(f_n + q_n) = 0. \quad (3.4)$$

Projecting Eq. (3.4) in the $\langle f'_n |$ direction yields

$$\begin{aligned} \ddot{X} = & -\frac{1}{M} [\langle f'_n | \ddot{q}_n + \Delta q_n \rangle + \dot{X}^2 \langle f'_n | f''_n \rangle \\ & + \langle f'_n | \Delta f_n - \omega_0^2 \sigma(f_n + q_n) \rangle], \end{aligned} \quad (3.5)$$

where $M = \langle f'_n | f'_n \rangle / l$ is the kink mass. Equation (3.5) is the equation of motion for the variable \bar{X} , the center of mass of the kink. We consider the trapped case and we proceed to calculate the zeroth-order frequency, which neglects the radiations emitted by the kink.

B. Zeroth-order PN frequency

Since simulation shows that the radiation emitted by the kink undergoing small-amplitude oscillations is negligible, we can take $q_n = 0$. Effects of the order \dot{X}^2 are also negligible for small-amplitude oscillations and so we set $\dot{X}^2 = 0$. We consider small-amplitude oscillations about Φ_n^s and choose f_n to be Φ_n^s [Eq. (2.10)]. Equation (3.5) becomes

$$\ddot{X} = -\frac{1}{M} [B_1 \langle \Phi_n^s | \Phi_n^s \rangle - K_1 (\langle \Phi_n^s | \Phi_{n-1}^s \rangle + \langle \Phi_n^s | \Phi_{n+1}^s \rangle) - \omega_0^2 \langle \Phi_n^s | \sigma(n-X) \rangle]. \quad (3.6)$$

By decomposing X as $X = \text{Int}(X) + R_X$, as done in Sec. II B, we explicitly calculate all the terms in the right-hand side of Eq. (3.6). Thus,

$$\langle \Phi_n^s | \sigma(n-X) \rangle = -2\nu^{1/2} Z_\nu \frac{\ln \nu}{1-\nu} \sinh\{(R_X - \frac{1}{2}) \ln \nu\}, \quad (3.7a)$$

$$\langle \Phi_n^s | \Phi_n^s \rangle = 2Z_\nu \ln \nu \left[\frac{Z_\nu \nu}{1-\nu^2} \sinh\{(2R_X - 1) \ln \nu\} - \frac{\nu^{1/2}}{1-\nu} \sinh\{(R_X - \frac{1}{2}) \ln \nu\} \right], \quad (3.7b)$$

$$\langle \Phi_n^s | \Phi_{n-1}^s \rangle + \langle \Phi_n^s | \Phi_{n+1}^s \rangle = 4Z_\nu \ln \nu \left[\frac{Z_\nu \nu^2}{1-\nu^2} \sinh\{(2R_X - 1) \ln \nu\} - \frac{\nu^{3/2}}{1-\nu} \sinh\{(R_X - \frac{1}{2}) \ln \nu\} \right], \quad (3.7c)$$

$$M \equiv M(X) = \frac{\nu Z_\nu^3 \ln^2 \nu}{d(1-\nu)^2} \cosh\{(2R_X - 1) \ln \nu\}. \quad (3.7d)$$

Note that the right-hand side of Eq. (3.6) is a periodic function of X since it depends only on R_X , because of the R_X dependence of Eqs. (3.7a)–(3.7d). It is also interesting to note that for $\gamma \rightarrow \infty$, i.e., $\nu \sim 1 - 1/\gamma$, $Z_\nu \sim 1$, the kink mass becomes

$$M \rightarrow 1/d, \quad (3.8)$$

where $1/d = \omega_0/C_0$ is the mass in the continuum limit, obtained in Ref. 24.

We expand Eq. (3.6) about the equilibrium, which

yields

$$\ddot{X} = -\omega_0^2(1+\nu)(R_X - \frac{1}{2})l. \quad (3.9)$$

By setting $X = m + \frac{1}{2} + \eta$ (that is, $R_X = \frac{1}{2} + \eta$), and linearizing in η , Eq. (3.9) becomes simply

$$\ddot{\eta} = -\bar{\omega}_{\text{PN}}^2 \eta, \quad (3.10)$$

where

$$\bar{\omega}_{\text{PN}} = (1+\nu)^{1/2} \omega_0 \quad (3.11)$$

represents the zeroth-order PN frequency of the DQ kink. This frequency always lies in the phonon band (since $0 < \nu < 1$), in contrast to the SG (Ref. 2) or ϕ^4 (Ref. 11) cases, for which the frequency is in the gap. The behavior of $\bar{\omega}_{\text{PN}}$ is therefore in agreement with the peculiar result obtained from MDS, in Sec. IID, that the PN frequency for the DQ kink always lies in the phonon band. We emphasize that such a peculiar result is understood by invoking the fact that there is no bound state in the discrete system, so that the center-of-mass motion of the trapped kink is generated by a packet of phonons.

It is interesting to examine the behavior of $\bar{\omega}_{\text{PN}}$ as a function of γ . For sufficiently small values of γ , that is, in the case of extreme discreteness, $\nu \sim 0$ [see Eq. (2.6)] so that $\bar{\omega}_{\text{PN}} \sim \omega_0$. This is due to the fact that in this limit the spectrum of allowed frequencies ω_k —which depends on γ according to the dispersion law [Eq. (2.16)]—collapses essentially to ω_0 , so that the kink's center-of-mass motion is generated by a packet of phonons with frequencies $\omega_k \sim \omega_0$, which leads to $\bar{\omega}_{\text{PN}} \sim \omega_0$.

As γ increases, the phonon spectrum increases so that it becomes possible for some phonons with frequencies $\omega_k > \omega_0$ to contribute to generate the kink's center-of-mass motion—hence the slight increase of $\bar{\omega}_{\text{PN}}$ with γ . $\bar{\omega}_{\text{PN}}$ approaches $\omega_0 \sqrt{2}$ for large kink sizes.

Furthermore, as $0 < R_X < 1$, the right-hand side of Eq. (3.9) vanishes when $l \rightarrow 0$, so that in the continuum limit

Eq. (3.9) becomes

$$\ddot{X} = 0,$$

which corresponds effectively to the continuum behavior.²⁴

Thus, since there is no bound state in the discrete system, it is therefore clear that the DQ system spontaneously gives rise to a bound state, which corresponds to the Goldstone mode as soon as the PN potential vanishes, whereas for the SG or ϕ^4 systems there always exist bound states (associated with the center-of-mass mode) as well in the discrete system as in the continuum limit. Note that for the DQ model, the Goldstone mode is not the limiting behavior of $\bar{\omega}_{\text{PN}}$ in the continuum limit: $\bar{\omega}_{\text{PN}}$ describes the behavior of a phonon packet, and is not associated to a bound state.

C. Numerical solutions of the collective-variable equations of motion

To determine exactly the PN frequency for all γ , we need to take into account the q_n 's. The coupled set of equations (3.4) and (3.5) are sufficient to determine the time evolution of X and q_n starting from some specified initial conditions. However, in each of these equations there appear two accelerations: \ddot{X} and \ddot{q}_n . Since we must solve Eqs. (3.4) and (3.5) numerically, it is desirable to have the acceleration of either variable be determined by a source that is a function of the coordinates and velocities and not on the other accelerations. The term $\langle f'_n | \ddot{q}_n \rangle$ in Eq. (3.5) is replaced by taking the second time derivative of C_1 , and solving for $\langle f'_n | \ddot{q}_n \rangle$ to obtain³⁷

$$\langle f'_n | \ddot{q}_n \rangle = -\ddot{X} \langle f'_n | q_n \rangle - \dot{X}^2 \langle f'''_n | q_n \rangle - 2\dot{X} \langle f''_n | \dot{q}_n \rangle. \quad (3.12)$$

Substituting Eq. (3.12) into (3.5), and thus eliminating the explicit acceleration dependence in the term $\langle f'_n | \ddot{q}_n \rangle$, yields

$$\ddot{X} = \frac{1}{\langle f'_n | f'_n \rangle - \langle f''_n | q_n \rangle} [-\langle f'_n | \Delta f_n + \Delta q_n \rangle + 2\dot{X} \langle f''_n | \dot{q}_n \rangle + \dot{X}^2 (\langle f'''_n | q_n \rangle - \langle f'_n | f''_n \rangle) + \omega_0^2 \langle f'_n | \sigma(f_n + q_n) \rangle]. \quad (3.13)$$

Solving Eq. (3.4) for \ddot{q}_n one obtains

$$\ddot{q}_n = -[\ddot{X} f'_n + \dot{X}^2 f''_n + \Delta q_n + \Delta f_n - \omega_0^2 \sigma(f_n + q_n)], \quad (3.14)$$

where the value of \ddot{X} obtained from Eq. (3.13) is to be substituted into the right-hand side of Eq. (3.14). Note that these equations govern the motion of the kink whether the kink is trapped or untrapped. We will solve the collective-variable (CV) equations of motion by using the numerical technique reported in Ref. 2.

We first address the problem related to the choice of ansatz function $f_n(X)$. As the quasistatic solution $\psi_n(X)$ [Eqs. (2.24) and (2.26)] provides a highly accurate representation of the shape of the kink for all X , a natural

choice would be $f_n(X) = \psi_n(X)$. [Note that we can no longer choose $f_n(X)$ to be Φ_n^s as we did previously for calculating the zeroth-order PN frequency, or even Φ_n^u , because these functions accurately represent the shape of the kink solely near the equilibrium states at the bottom and the top of the PN well, respectively.] However, solving the CV equations of motion (3.13) and (3.14) necessitates working out the derivative of the ansatz function up to the third order. The derivatives of $\psi_n(X)$ possess terms which contain the Dirac δ function and its derivatives δ' and δ'' , which must be taken into account to obtain the exact solutions for the collective variables X and q_n . As long as the kink oscillates within the PN well and does not reach its summit (trapped case) the

δ , δ' , and δ'' terms vanish, so that one can choose the ansatz $f_n(X) = \psi_n(X)$ for the CV theory. However, for the untrapped case, the δ , δ' , and δ'' terms yield nonzero contributions to the CV equations of motion when the kink passes over the top of the PN well, precisely when $X = n$, where n is a site index. So, solving numerically Eqs. (3.13) and (3.14) in the presence of the δ , δ' , and δ'' terms, *directly*, is very cumbersome. Although one can transform these equations by using Fourier transform techniques and obtain equations which do not contain the δ , δ' , and δ'' terms,³⁸ we do not choose this method of attack. In fact, in the context of CV theory, it is not truly necessary to choose ψ_n to be the ansatz function. Any choice of f_n that suitably represents the configuration of the system will do as long as the q_n are fully taken into account.³⁶ So, for numerically solving the Eqs. (3.13) and (3.14), for all regimes of the discrete kink's motion, we choose the following ansatz function:

$$f_n(X) = \tanh[\lambda(n - X)] , \quad (3.15)$$

where the factor λ is as yet an unknown quantity, which represents the width of the stationary kink described by $f_n(X)$. The ansatz Eq. (3.15) is the well-known configuration of a ϕ^4 kink in the continuum limit,^{9,14} where we have replaced the continuous position variable x by the site index n . This ansatz has been used already by Combs and Yip¹¹ for the study of the dynamics of the ϕ^4 kink within the CV formalism. There is no need to explicitly include a relativistic factor $\beta(t)$ multiplying λ in Eq. (3.15), because any relativistic effects will necessarily be taken into account by the q_n .¹ We choose λ to be of the form

$$\lambda = -\xi \ln v , \quad (3.16)$$

where $\ln v$ makes the relationship between $f_n(X)$ and our discreteness parameter γ by requiring $f_n(X)$ to have the same argument $[\lambda(n - X)]$ as that of our quasistatic solution ψ_n ; the minus sign is required to have $\lambda > 0$. ξ is a factor which makes $f_n(X)$ a best fit to the initial configuration of the kink $\psi_n(X(t=0))$. The meaning of ξ will be made more mathematically precise in the following discussion.

The initial conditions start with a kink that is relaxed to one of the equilibrium configurations along the PN potential, $X_0 \equiv X(t=0) = N/2$, with a given initial velocity $V_0 \equiv \dot{X}(0)$, so that X_0, V_0 ,

$$Q_n(0) = \psi_n(X_0) , \quad (3.17)$$

and

$$q_n(0) = Q_n(0) - f_n(X_0) \quad (3.18)$$

are known for a given ξ . Furthermore, it is important to note that the initial conditions for the collective-variable theory (CVT) must satisfy the constraint conditions in Eqs. (3.3) at $t=0$. The CVT then guarantees that the constraints will be zero for all time.¹ As the initial kink profile is centered on an equilibrium point of the PN potential, $q_n(0)$ is odd and consequently $C_1(0) = 0$ whatever ξ , since $f'_n(X_0)$ is even. However, it is crucial to note

that the fact that $C_1(0) = 0$ does not imply that any choice of ξ , for f_n , will do. Indeed the idea in introducing the first constraint condition $C_1(0) = 0$ is to make the CVT lead to the determination of the value of X for which the ansatz function $f_n(X)$ is the best fit to the field Q_n , for all time t and in particular for $t=0$. That is, the extremum of

$$\sum_n q_n^2 = \sum_n [Q_n - f_n(X)]^2 \quad (3.19)$$

with respect to X yields $C_1(t) = 0$. Similarly, we obtain the parameter ξ in Eq. (3.16) by requiring the ansatz function $f_n(X)$ in Eq. (3.15) to be the best fit to the field $Q_n \equiv \psi_n(X_0)$ at $t=0$:

$$\frac{d}{d\xi} \sum_n [\psi_n(X_0) - f_n(X_0)]^2 = 0 , \quad (3.20)$$

which leads directly to the following equation for ξ :

$$\sum_n \{ \psi_n(X_0) - \tanh[(X_0 - n)\xi \ln v] \} \{ n - X_0 \} \\ \times \{ 1 - \tanh^2[(X_0 - n)\xi \ln v] \} = 0 . \quad (3.21)$$

Equation (3.21) admits exactly one solution ξ , for a given γ , and this solution minimizes the quantity in Eq. (3.19). Note that Eq. (3.21) differs from the first constraint condition $C_1(0) = 0$ by the presence of the factor $\{n - X_0\}$. [Equation (3.20) is in fact the first constraint condition for the variable ξ if we were to treat ξ as a collective variable. However, in the present paper we do not treat ξ as a collective variable, but rather as a constant, whose value we obtain from Eq. (3.21) at $t=0$.]

In order to illustrate that the center-of-mass mode for the DQ kink is a well-defined collective entity [in the sense that its collective coordinate X possesses exact equations of motion, given by Eqs. (3.13) and (3.14)], we will systematically choose the same initial conditions for the CVT and MDS and compare our results in the two cases. This necessitates constructing a map from the MDS initial conditions $[Q_n(0), \dot{Q}_n(0)]$ onto the CVT initial conditions $[q_n(0), \dot{q}_n(0), X_0, \text{ and } V_0]$. We consider in the present work the map derived in Ref. 2, which is constructed in a way such that the condition $C_2(0) = 0$ is always satisfied whatever the initial velocity; consequently, this map² can be systematically used whether the kink is trapped or untrapped. This map is then given by the following equations:^{2,37}

$$\dot{Q}_n(0) = \frac{\alpha}{\Delta t} f'_n(X_0) , \quad (3.22)$$

$$V_0 = \frac{\alpha/\Delta t}{1-b(0)} , \quad b(0) = \frac{\langle f''_n(X_0)/q_n(0) \rangle}{M(X_0)} . \quad (3.23)$$

$$\dot{q}_n(0) = -b(0)V_0 f'_n(X_0) , \quad (3.24)$$

where the $q_n(0)$ are obtained from Eq. (3.18), and α is a small parameter.

Figure 5(b) shows the numerical solution of Eqs. (3.13) and (3.14) for the case $V_0 = 0$ discussed in Sec. II D—*a*

kink of $\gamma=1$ trapped and oscillating in the PN well. For $\gamma=1$, $\xi=0.70898$. During the numerical solution of the Eqs. (3.13) and (3.14) the magnitude of the constraints C_1 and C_2 does not exceed 1.5×10^{-5} and 2.5×10^{-5} , respectively; the energy of the system is conserved to an accuracy better than $1.3 \times 10^{-4}\%$. During this trapped motion we note that the kink radiates in forward and backward directions [Figs. 5 (e) and 5 (f)] essentially in a similar fashion, and does not undergo appreciable distortion during this trapped motion. Throughout the simulation the MDS and the CVT yield essentially the same result for the field variable Q_n , but for simplicity we only give in Figs. 5(e) and 5(f) the kink profile at $t=t_f \approx 1065$; [typically we find that $Q_n^{\text{CVT}}(t_f) = Q_n^{\text{MDS}}(t_f) \pm 10^{-10}$; recall that $Q_n^{\text{CVT}}(t) = f_n(X) + q_n(t)$]. Figure 5 shows that the CVT results agree extremely well with MDS results (see the Appendix for more details on the evaluation of the agreement between the collective-variable result X_{CVT} and the MDS result X_{MDS}). Since the trapped process has been discussed in detail in Sec. II D, we now turn to

the untrapped case.

Our MDS and CVT for the untrapped case with $\gamma=10$ and $\alpha=0.0075$ (which corresponds to $V_0=0.079C_0$) appear in Figs. 7. For $\gamma=10$, $\xi=0.71695$. Both simulation and theory start with a kink—in a chain of 4000 particles—at the top of the PN well No. 2000 moving in the positive x direction. During the numerical solution of the Eqs. (3.13) and (3.14), $C_1(t)$ and $C_2(t)$ do not exceed 9.5×10^{-9} and 1.5×10^{-8} , respectively. The energy of the system is conserved in an accuracy better than $8 \times 10^{-3}\%$. We see in Figs. 7(c) and 7(d) that when the kink begins its motion, its velocity continually decreases, indicating that the kinetic energy of the kink is radiated away in the form of phonons. The kink then slows down as it radiates, until it becomes trapped. After trapping, the ensuing motion is the same as that discussed in Sec. II D.

The behavior of the untrapped ϕ^4 (Ref. 11) and SG (Refs. 2 and 39) kinks has been studied in great detail. One of the main results of these studies is that when the initial velocity is large enough, the untrapped motion leads to bends in the curves of the kink's velocity versus time, which appear at critical velocities, at which the radiative damping changes abruptly. For our simulations, one of these velocities is found to be ~ 2.2 for ($\gamma=10$, $V_0=0.079C_0$); but this is not visible in Fig. 7 because the initial velocity V_0 is not large enough. We have not investigated this problem in more detail in the present paper, and we have always chosen relatively small initial velocities in order that the kink becomes quickly trapped.

We now turn our attention to limiting cases, that is, the case of extreme discreteness and the case where discreteness effects become negligible. We briefly discuss separately the two cases:

(i) In the case of extreme discreteness, the *trapping* dominates: Whatever V_0 , the kink is quickly trapped. We see in Figs. 8, which show the results obtained for $\gamma=1$ and $\alpha=0.0275$ (which corresponds to $V_0=0.32C_0$), that the kink's dynamics in the trapped motion now differ significantly from the previous case ($\gamma=1$, $V_0=0$) where the kink is initially trapped in the PN well. Indeed, for the trapped case ($V_0=0$) the amplitude of oscillation is initially large [see Figs. 5(a) and 5(b)] and the shape of the kink does not undergo a significant distortion during the oscillatory motion, whereas for the untrapped case ($V_0 \neq 0$) the kink begins its trapped motion with a relatively small amplitude of oscillation [Fig. 8(a)], owing to the emission of a burst of phonon radiation during the transition from the ballistic propagation to the trapped regime. Figure 8(b) shows that this phonon radiation is much more strong than in the case ($V_0=0$) [Figs. 5(c) and 5(d)]. It is also interesting to note in Fig. 8(c) that the PN frequency appears in the phonon band as soon as the kink begins its trapped motion; $\omega_{\text{PN}}(t=0) \approx 1.18\omega_0$; which agrees extremely well with $\bar{\omega}_{\text{PN}}(\gamma=1) \approx 1.17\omega_0$ [see Eq. (3.11)]. Moreover, we recover the peculiar result (obtained from MDS in Sec. II D) that the PN frequency for the DQ kink is a monotonically decreasing function of time; which differs from all other known nonintegrable field theories. Furthermore, we

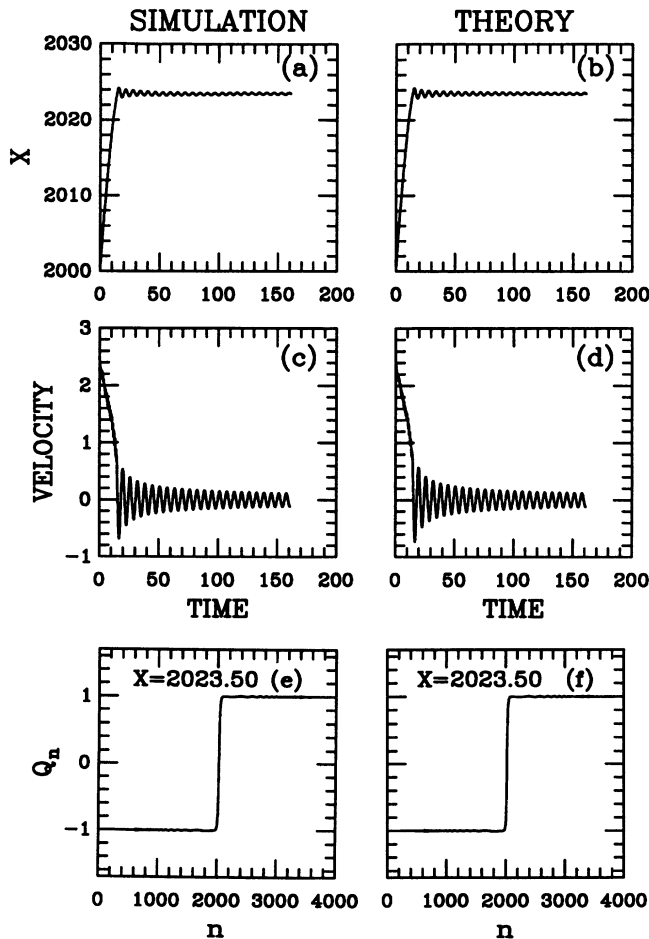


FIG. 7. Simulation and collective-variable theory for $\gamma=10$. (a) and (b): $X(t)$; (c) and (d): velocity; (e) and (f): kink profile at the end of the total time of the calculations, that is, at $t \equiv t_f \approx 160.8$. Simulation parameters are $\alpha=0.0075$ ($V_0 \approx 0.079C_0$), $\omega_0=1$, $C_0=30$, $l=3$, $\Delta t = \pi/1000$, and $X_0 = N/2 = 2000$.

see in Fig. 8(c) that the PN frequency at $t=0$, $\omega_{\text{PN}}(t=0)/\omega_0$, differs from that of the case ($V_0=0$) in Fig. 4; we attribute this difference between the PN frequencies to the differences in the kink's behavior at the beginning of the trapped motion, mentioned above. In this respect we notice that the shape of the untrapped kink undergoes appreciable distortions during the transition to the trapped regime and these distortions remain present in the trapped motion during a certain time, as shown in Fig. 8(d), and the kink does not radiate phonons in a similar fashion in backward and forward directions [Figs. 8(e)]. However, after a certain time depending on the initial velocity, the distortion of the kink progressively vanishes and the kink recovers a more steady profile

that is more close to its initial profile and radiates phonons in an almost similar fashion in backward and forward direction; the ensuing oscillatory motion is then similar to the case $V_0=0$.

(i) When the discreteness effects become sufficiently small, the kink travels on several hundred lattice spacings with a relatively constant velocity, as shown in Fig. 9 obtained for $\gamma=100$. The radiation emitted by the kink is found to be negligible.

Furthermore, for all the cases (γ, V_0) that we have discussed throughout the paper, we note excellent agreement between the CVT result for the kink's center of mass X_{CVT} and the result X_{MDS} obtained by using our quasistatic solution $\psi_n(X)$ (see the Appendix).

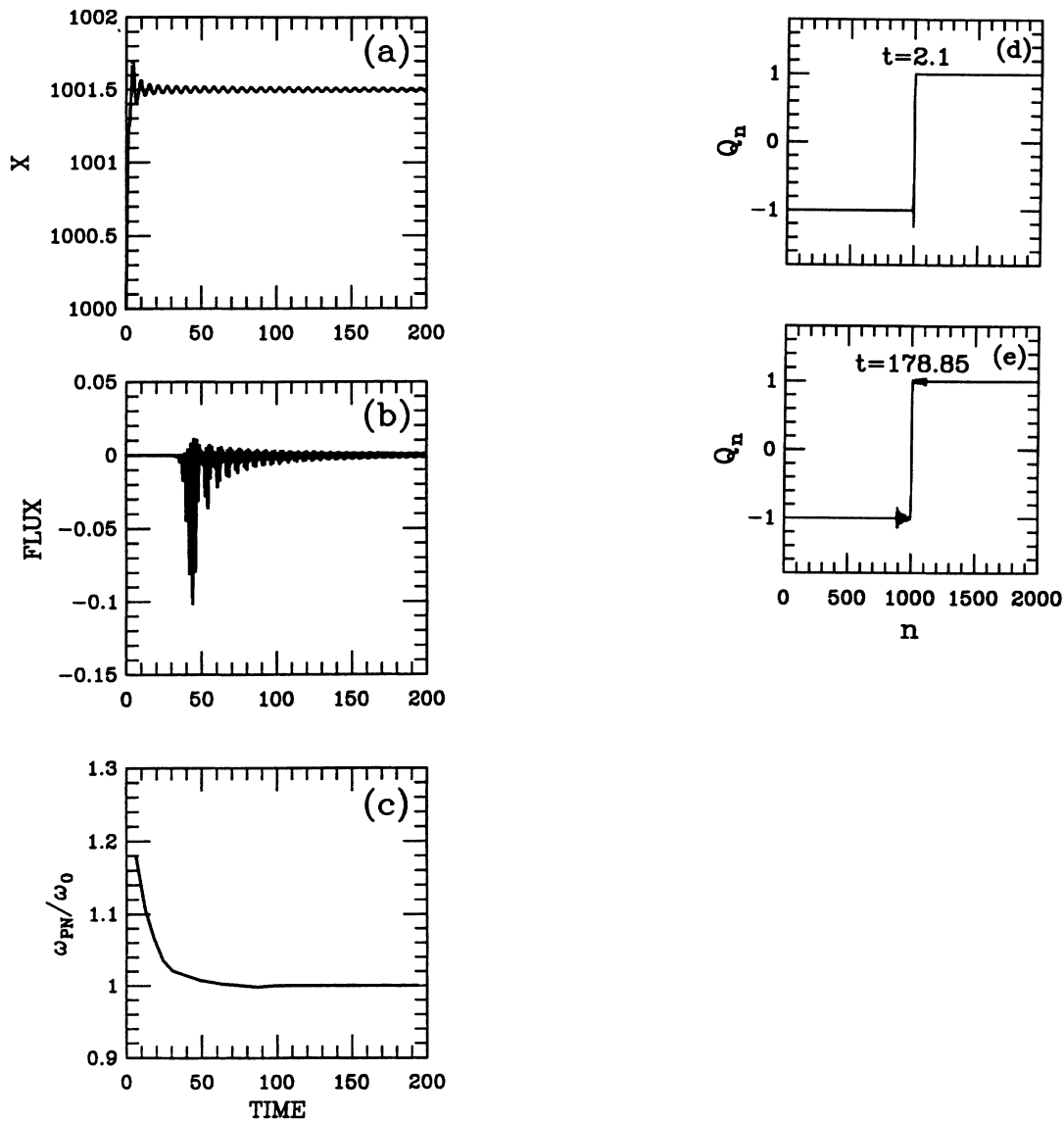


FIG. 8. Collective-variable theory for $\gamma=1$. (a) $X(t)$; (b) instantaneous Poynting's flux evaluated at $n=976$ in backward direction of moving kink; (c) normalized PN frequency of trapped kink motion over individual cycles; (d) shows the kink profile at $t \equiv t_1 = 2.1074$ [$X(t_1) = 1001.25$]; (e) the kink profile at $t \equiv t_2 = 178.75$. Simulation parameters are $\alpha = 0.0275$ ($V_0 \approx 0.32$), $\omega_0 = 1$, $C_0 = 3$, $l = 3$, $\Delta t = \pi/111.5$, and $X_0 = N/2 = 1000$.

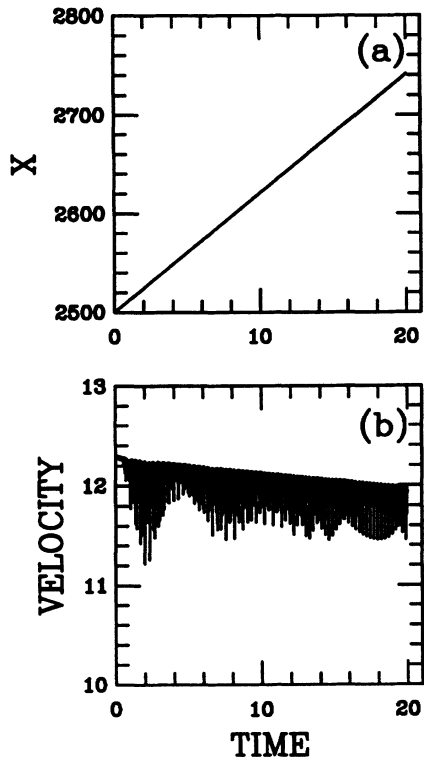


FIG. 9. Molecular-dynamic simulations for $\gamma = 100$. (a) $X(t)$; (b) velocity. Simulation parameters are $\alpha = 0.004$ ($V_0 \approx 0.042C_0$), $\omega_0 = 1$, $C_0 = 300$, $l = 3$, $\Delta t = \pi/10^4$, and $X_0 = N/2 = 2500$.

IV. SUMMARY AND CONCLUSION

In the present paper we have studied static and dynamic properties of the discrete DQ kink. We have shown that the zeroth-order PN frequency always lies in the phonon band whatever the discreteness parameter may be. The presence of the PN frequency in the band is in marked contrast with other discretized field theories. This is because the presence of the kink in the DQ system does not give rise to a scattering localized potential acting on the phonons. Consequently there is no bound state and localized state about the kink, and by Levinson's theorem³¹ there is no phase shift of a phonon as it traverses the kink. We have shown that the DQ kink possesses all regimes of the discrete kink's motion: the untrapped regime and the trapped regime. For the trapped case we observe that, when the kink begins a large-amplitude oscillatory motion, its frequency of oscillations is slightly greater than the limiting frequency of wavelength phonons ω_0 . This frequency quickly decreases in time, while the kink strongly radiates away a large phonon packet. Next the kink reaches a steady state in which the phonons are now radiated weakly and in a smooth fashion and the ensuing oscillatory motion is almost perfectly harmonic, at frequency ω_0 . However, we stress that the center-of-mass mode is not a nonlinear mode, but rather a quasimode in the same sense as is the shape mode³³ of a sine-Gordon kink.

We have demonstrated in the present paper that although the discrete DQ system does not possess a nonlinear mode, the discrete DQ kink behaves like a well-defined collective entity whose center of mass can be described within a collective-variable formalism. Thus, as the description of commensurate phases in one-dimensional DQ systems can be reduced to that of a finite number of domain walls embedded within a periodic unit cell,²² our study suggests that the dynamics of those commensurate phases can be described within a collective-variable formalism where the collective variables represent the distances between the domain walls, or, equivalently, their positions. The dynamics of those domain walls can induce phase transitions, and, then, involve the propagation of phase fronts along the lattice. As the phase fronts are spatially localized entities, they could therefore be described theoretically in a collective-

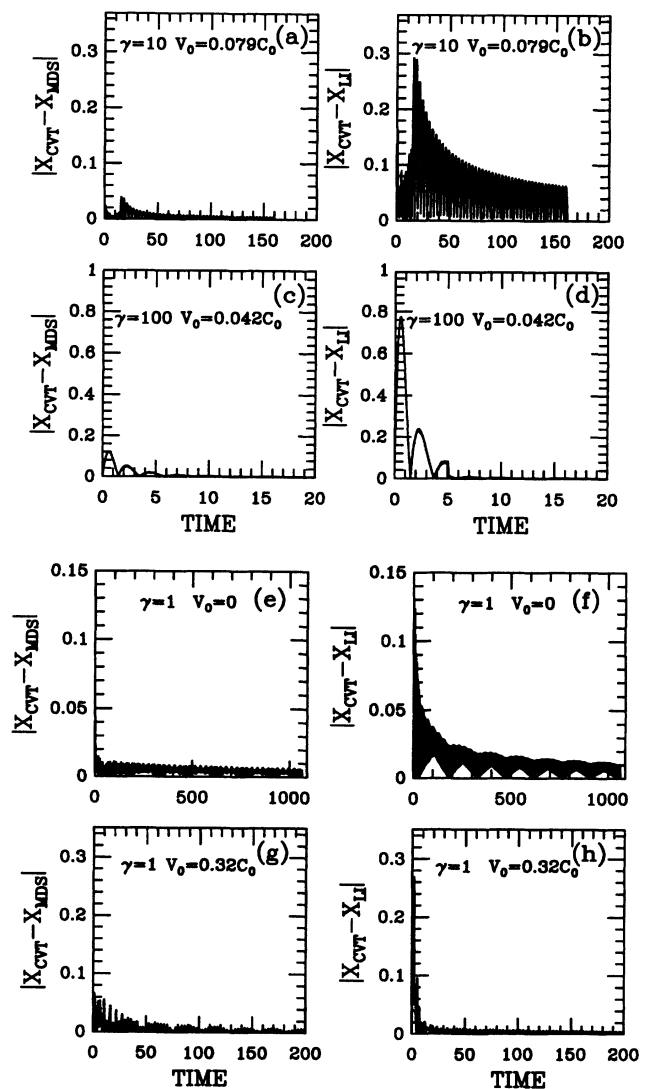


FIG. 10. Evaluation of the agreement between the results for $X_{CVT}(t)$ and $X_{MDS}(t)$, and between $X_{CVT}(t)$ and $X_{LI}(t)$. (a) and (b): for $\gamma = 10$, $V_0 = 0.079C_0$; (c) and (d): for $\gamma = 100$, $V_0 = 0.042C_0$; (e) and (f): for $\gamma = 1$, $V_0 = 0$; (g) and (h): for $\gamma = 1$, $V_0 = 0.32C_0$.

variable context. In this respect, our study of a single-kink bearing system, without making use of the continuum limit approximation, appears as an encouraging step in this direction.

Furthermore, it is well known that the motion of the domain walls can make measurable contributions to the dynamic properties of various materials, such as the presence of a central peak in the dynamic structure factor due to domain walls, in some ferroelectric materials.^{10,40} The ϕ^4 and SG fields are usually used for the description of the properties of such materials in which the crystalline anharmonicity gives rise to one or more bound states associated with the presence of the domain walls in the system.^{9,10,12,14} These bound states induce phase shift for phonons upon passing through the crystal.³¹ However, the present work shows that the DQ field is a candidate for the study of systems in which the domain walls do not phase shift phonons.

ACKNOWLEDGMENT

We wish to thank M. Peyrard for helpful discussions.

APPENDIX

In the present work, we have used a simple method for obtaining the kink's center of mass from MDS, which utilizes the quasistatic kink solution ψ_n [Eq. (2.24) and

(2.26)]. In this Appendix we compare this method with the linear interpolation (LI) procedure—which has been used in previous work²—and we show that some care must be taken in comparing the results of the CVT for X with the results obtained by measuring X from other methods.

We have systematically found that $Q_n^{\text{CVT}}(t) = Q_n^{\text{MDS}}(t) \equiv Q_n(t)$; moreover, we see in Fig. 10, where we evaluate the agreement between the CVT and the LI on the one hand, and on the other hand, the agreement between the CVT and our MDS procedure, that $|X_{\text{CVT}}(t) - X_{\text{MDS}}(t)|$ does not exceed 0.07 for all the cases γ that we have considered, whereas the maximum value of $|X_{\text{CVT}}(t) - X_{\text{LI}}(t)|$ attains essentially 0.3 for $\gamma=10$ [Fig. 10(b)] and 0.8 for $\gamma=100$ [Fig. 10(d)]. This slight difference between some CVT and LI results is not specific to the DQ model. Indeed, we also observe a slight difference between the CVT and LI results in Fig. 3 in Ref. 2, for the amplitudes of oscillations of a trapped SG kink. We attribute these slight differences to the approximate nature of the LI procedure, because this method takes into account only two of the particles that make up the kink—for obtaining its center of mass [see Eq. (2.29)], which, by the way, must not be ignored in doing a comparison between the CVT and LI results. Furthermore, Fig. 10 shows in general that the results of the CVT agree much better with our MDS results than do the LI results.

¹R. Boesch, P. Stancioff, and C. R. Willis, *Phys. Rev. B* **38**, 6713 (1988).
²R. Boesch, C. R. Willis, and M. El-Batanouny, *Phys. Rev. B* **40**, 2284 (1989).
³R. Boesch and C. R. Willis, *Phys. Rev. B* **39**, 361 (1989).
⁴R. Boesch and M. Peyrard, *Phys. Rev. B* **43**, 8491 (1991).
⁵C. R. Willis and R. Boesch, *Phys. Rev. B* **41**, 4570 (1990).
⁶M. Taki, J. C. Fernandez, and G. Reinisch, *Phys. Rev. A* **38**, 3086 (1988).
⁷D. K. Campbell, M. Peyrard, and P. Sodano, *Physica* **19D**, 165 (1986).
⁸R. Ravelo, M. El-Batanouny, C. R. Willis, and P. Sodano, *Phys. Rev. B* **38**, 4817 (1988).
⁹S. Aubry, *J. Chem. Phys.* **64**, 3392 (1976).
¹⁰S. Aubry, Ph.D. thesis, University of Paris VI, 1975 (unpublished), and references therein.
¹¹J. Andrew Combs and Sidney Yip, *Phys. Rev. B* **28**, 6873 (1983).
¹²M. A. Collins, A. Blumen, J. F. Currie, and J. Ross, *Phys. Rev. B* **19**, 3630 (1979).
¹³D. Hochstrasser, H. Büttner, H. Desfontaines, and M. Peyrard, *Phys. Rev. A* **38**, 5332 (1988), and references therein.
¹⁴J. A. Krumhansl and J. R. Schrieffer, *Phys. Rev. B* **11**, 3535 (1975).
¹⁵Y. Wada and J. R. Schrieffer, *Phys. Rev. B* **18**, 3897 (1978).
¹⁶W. Kob and R. Schilling, *Phys. Rev. A* **42**, 2191 (1990).
¹⁷F. Axel and S. Aubry, *J. Phys. C* **14**, 5433 (1981).
¹⁸M. Peyrard and H. Büttner, *J. Phys. C* **20**, 1535 (1987).
¹⁹P. Reichert and R. Schilling, *Phys. Rev. B* **32**, 5731 (1985).

²⁰P. Tchofo Dinda and E. Coquet, *J. Phys. Condens. Matter* **2**, 6953 (1990).
²¹P. Tchofo Dinda and E. Coquet, *J. Phys. Condens. Matter* **3**, 7587 (1991).
²²P. Tchofo Dinda, Ph.D. thesis, University of Dijon, 1991 (unpublished).
²³S. E. Trullinger, *J. Math. Phys.* **21**, 592 (1980).
²⁴S. E. Trullinger and R. M. DeLeonardis, *Phys. Rev. A* **20**, 2225 (1979).
²⁵M. Peyrard, *J. Math. Phys.* **22**, 2986 (1981).
²⁶A. Seeger and P. Schiller, *Phys. Acoust.* **III**A, 361 (1966).
²⁷P. A. Lee, T. M. Rice, and P. W. Anderson, *Solid State Commun.* **14**, 703 (1974).
²⁸A. R. Bishop, *J. Phys. C* **11**, 5433 (1971).
²⁹A. Bestaoui, Ph.D. thesis, University of Dijon, 1985 (unpublished).
³⁰J. Bornarel, *Ferroelectrics* **71**, 255 (1987).
³¹K. Gottfried, *Quantum Mechanics, Volume I: Fundamentals* (Benjamin, New York, 1966), pp. 394—396.
³²P. A. M. Dirac, *Lectures on Quantum Mechanics* (Academic, New York, 1964).
³³R. Boesch and C. R. Willis, *Phys. Rev. B* **42**, 2290 (1990).
³⁴C. M. Bender and S. A. Orszag, *Advanced Mathematical Methods for Scientists and Engineers* (McGraw-Hill, New York, 1986), pp. 49–53.
³⁵We obtain the frequency spectrum by proceeding as in previous works (Refs. 2 and 4); we calculate the magnitude of the temporal Fourier transform of each of the 50 center particles of the chain that contain the kink. We construct a matrix of

frequency versus particle number, thereby forming relief of the transform and normalizing the largest peak in the matrix to unity. Choosing a cutoff between 0 and 1, we plot a point for each peak in the relief matrix whose magnitude exceeds the cutoff value.

³⁶R. Boesch and C. R. Willis, *Phys. Rev. B* **42**, 6371 (1990).

³⁷Note that the prime of the f_n in Ref. 2 is the derivative with respect to $(n - X)$, whereas in the present paper the prime is

the derivative with respect to X .

³⁸N. Flytzanis, Ph.D. thesis, University of Virginia, 1971 (unpublished); V. Celli and N. Flytzanis, *J. Appl. Phys.* **41**, 4443 (1970).

³⁹M. Peyrard and M. D. Kruskal, *Physica* **14D**, 88 (1984).

⁴⁰M. A. Collins, A. Blumen, J. F. Currie, and J. Ross, *Phys. Rev. B* **19**, 3630 (1979).